European Journal of Medicinal Chemistry 249 (2023) 115147

Contents lists available at ScienceDirect

European Journal of Medicinal Chemistry

journal homepage: www.elsevier.com/locate/ejmech

Research paper

Investigation of tetrasubstituted heterocycles reveals hydantoins as a promising scaffold for development of novel antimicrobials with membranolytic properties

Manuel K. Langer [a], Ataur Rahman [b], Hymonti Dey [b], Trude Anderssen [c], Hans-Matti Blencke [b], Tor Haug [b], Klara Stensvåg [b], Morten B. Strøm [c,*], Annette Bayer [a,*]

[a] Department of Chemistry, UiT – The Arctic University of Norway, NO-9037, Tromsø, Norway
[b] The Norwegian College of Fishery Science, Faculty of Biosciences, Fisheries and Economics, UiT – The Arctic University of Norway, NO-9037, Tromsø, Norway
[c] Department of Pharmacy, Faculty of Health Sciences, UiT – The Arctic University of Norway, NO-9037, Tromsø, Norway

ARTICLE INFO

Keywords:
Antimicrobial peptides (AMP)
Synthetic mimics of antimicrobial peptides (SMAMPs)
Peptidomimetics
Hydantoin
Membranolytic

ABSTRACT

Mimics of antimicrobial peptides (AMPs) have been proposed as a promising class of antimicrobial agents. We report the analysis of five tetrasubstituted, cationic, amphipathic heterocycles as potential AMP mimics. The analysis showed that the heterocyclic scaffold had a strong influence on the haemolytic activity of the compounds, and the hydantoin scaffold was identified as a promising template for drug lead development. Subsequently, a total of 20 hydantoin derivatives were studied for their antimicrobial potency and haemolytic activity. We found 19 of these derivatives to have very low haemolytic toxicity and identified three lead structures, **2dA**, **6cG,** and **6dG** with very promising broad-spectrum antimicrobial activity. Lead structure **6dG** displayed minimum inhibitory concentration (MIC) values as low as 1 μg/mL against Gram-positive bacteria and 4–16 μg/mL against Gram-negative bacteria. Initial mode of action (MoA) studies performed on the amine derivative **6cG**, utilizing a luciferase-based biosensor assay, suggested a strong membrane disrupting effect on the outer and inner membrane of *Escherichia coli*. Our findings show that the physical properties and structural arrangement induced by the heterocyclic scaffolds are important factors in the design of AMP mimics.

1. Introduction

Antimicrobial resistance is now considered to have a similar impact on humans as global climate change [1]. Despite that, only around 30–40 new antimicrobial agents are currently in clinical trials and they are mainly derivatives of already marketed compound classes [2]. To combat the rising resistance, new and underdeveloped classes of compounds have to be utilized.

One promising group of antibiotic agents are the naturally occurring cationic antimicrobial peptides (AMPs), found in practically all higher forms of life [3]. Their amphipathic nature allows them to associate with the negatively charged bacterial outer membrane simultaneously as the lipophilic residues can insert and disrupt the membrane [3]. It is believed that due to the lack of a specific target, AMPs are less likely to induce antibiotic resistance development [4]. However, proteolytic instability [5], sometimes tedious synthetic procedures [6] and moderate activity [4] are among the drawbacks AMPs have been facing, thus retarding their development. To address these issues a range of synthetic AMP analogues have been reported including peptoids [7,8], oligoureas [9], γ-AApeptides [10,11] and other small synthetic mimics of antimicrobial peptides (SMAMPs) [6,12,13].

In recent years, we have focussed on the development of synthetic analogues of AMPs that fulfil and operate at the limit of the pharmacophore model for AMPs. That is, the presence of two cationic groups and two lipophilic groups of sufficient bulk to exert broad-spectrum activity [14]. Among these were β-amino amides [15,16], cyclic tetrapeptides [16], barbiturates [17] and others [18,19]. The barbituric acid framework **1** has proven to be a valuable scaffold for the preparation of highly active antimicrobials [17,20], and we were curious if our previous results would translate to other scaffold structures.

In this work we initially investigated five heterocyclic scaffolds **2–5** and **15** (Fig. 1), that would allow for the same substitution pattern of two lipophilic side chains and two cationic chains as demonstrated for barbituric acid **1** [17,20]. To achieve segregation of the cationic and

* Corresponding authors.
E-mail addresses: morten.strom@uit.no (M.B. Strøm), annette.bayer@uit.no (A. Bayer).

https://doi.org/10.1016/j.ejmech.2023.115147
Received 13 November 2022; Received in revised form 19 December 2022; Accepted 21 January 2023
Available online 24 January 2023

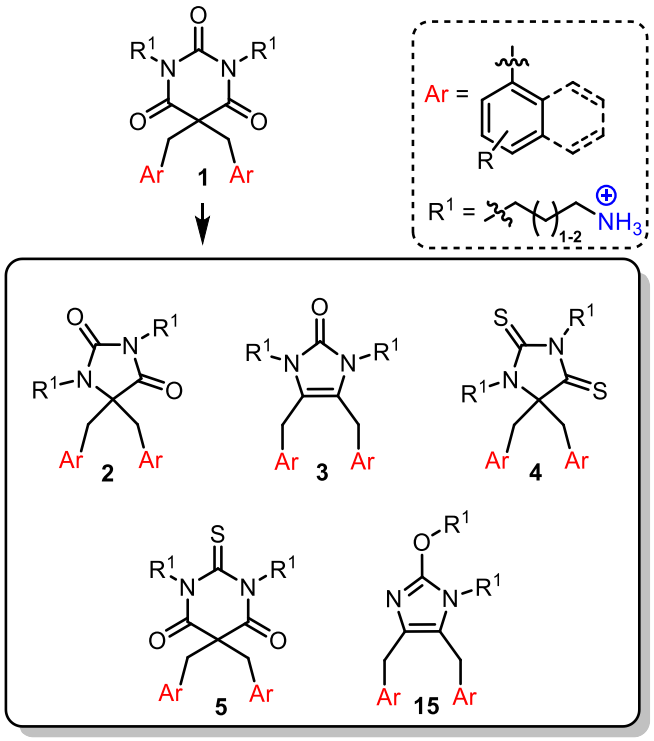

Fig. 1. Previously utilized barbituric acid **1** and core structures **2–5** and **15** used in this study. Ar = lipophilic side chain, R^1 = *n*-alkyl linker with a cationic head group. Red: lipophilic part, blue: cationic part.

lipophilic part we intended to attach the lipophilic side chains (Ar) at the bottom side of the heterocycles, bound to carbon atoms (Fig. 1). The *n*-alkyl linkers bearing the cationic head group (R^1) were incorporated onto the top side, bound to the nitrogen atoms (Fig. 1).

We then constructed a small library based on the most promising scaffold, the hydantoin **2**, and evaluated the effect of different lipophilic and cationic side chains. For the most potent analogues, their membranolytic behaviour was studied.

2. Results and discussion

2.1. Design of the study

We planned three sets of compounds. In the first set all core structures (**2–5** and **15**) shown in Fig. 1 were synthesized with a combination of substituents (Fig. 2, left) that we had evaluated in previous studies of amphipathic, antimicrobial barbituric acid derivatives [17,20].

Lipophilic 3,5-dibromobenzyl (3,5-di-Br) side chains were found earlier to be beneficial for the antimicrobial potency [16,17]. Aliphatic *n*-propyl linkers exhibited a good balance between antimicrobial potency and haemolytic activity [20] and amine groups were most accessible. It should be noted that we did not aim for the 2-(hydroxy)-1*H*-imidazole **15A** in the initial plan, but **15A** was obtained as a side product during synthesis. The second set was comprised of tetrasubstituted hydantoins **2** (Fig. 2, right) with different lipophilic side chains, *n*-propyl linkers, and amines and guanidines as cationic head groups. The lipophilic side chains and cationic groups were chosen based on their performance in previous studies [16,17,20,21]. For the third set we used promising lipophilic side chains from the second set and incorporated *n*-butyl linkers to deliver hydantoins **6** (Fig. 2, right). The *n*-butyl linkers have previously demonstrated to result in more potent derivatives [17,20].

Imidazolidine-2,4-dione **2**, commonly known as hydantoin, is a privileged scaffold in medicinal chemistry, found in drugs against

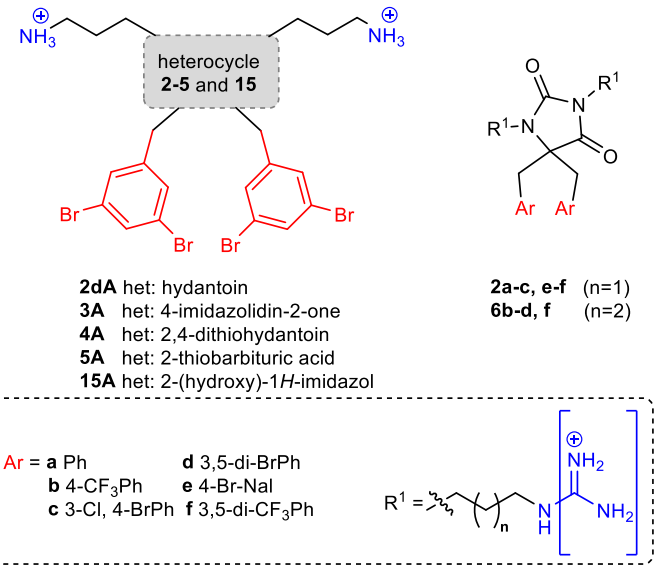

Fig. 2. Illustration of the three sets of compounds investigated. Brackets imply variations between cationic amine and guanidine groups.

various conditions [22–27]. However, it is only rarely seen in antimicrobial agents [6,28–30]. Of particular interest to this work, is a study by Cai and co-workers who demonstrated that suitably substituted hydantoins can effectively target bacterial membranes [6]. In the related 4-imidazolidin-2-one **3,** the lipophilic side chains were attached to two vicinal sp^2 hybridized carbons, providing more spatial separation and altered dihedral angle between the side chains. Additionally, removal of the amidic oxygen from hydantoin **2** led to a slight change in polarity. The changes in structure and physical properties may affect the compounds' ability to interact with the bacterial membrane. Lastly, we wanted to investigate the effect of sulphur on the biological activity. Thioamides are often utilized in peptide synthesis [31] and are known to hamper enzymatic degradation of peptides [32]. Sulphur is also found in a variety of different drugs [33,34], including some antimicrobial thio-peptides [35,36] and β-lactam antibiotics such as penicillins and cephalosporines [37]. In most of these structures the sulphur atom is part of a heterocyclic ring or a (di)sulfide, but not a thioamide or a related motif. Therefore, we were interested in joining those two areas by replacing some oxygens for sulphur atoms in the hydantoin and barbituric acid [17] core structures. The resulting structures were 2, 4-dithiohydantoin **4** and 2-thiobarbituric acid **5**.

2.2. Synthesis

2.2.1. Hydantoins *2* and *6*

The hydantoin structure can be accessed from a range of different reactions [38–41], including the Read [42], Bucherer-Bergs [43] and Biltz [44] syntheses. To achieve higher substitution patterns and to facile the access of compound libraries, modern strategies have been developed such as multicomponent reactions [45,46].

Based on the required substitution pattern and the nature of substituents, we decided to utilize the Bucherer-Bergs reaction as the key step in our synthetic strategy towards hydantoins **2A** and **6A** (Scheme 1). To that end, we prepared symmetric ketones **6** from *p*-toluenesulfonylmethyl isocyanate (TosMIC) **7** [47]. TosMIC was α,α-dialkylated using phase-transfer catalysis (PTC) in DCM and an aqueous NaOH solution with the benzyl bromide of choice. The crude products were hydrolysed by treatment with concentrated HCl [47] to give symmetric ketones **8(a–f)** in 53–69% yield over two steps (o2s). The Bucherer-Bergs reaction is commonly performed in a mixture of EtOH/H_2O [43], with precipitation of the resulting hydantoins as the main driving force. Unfortunately, only the unsubstituted

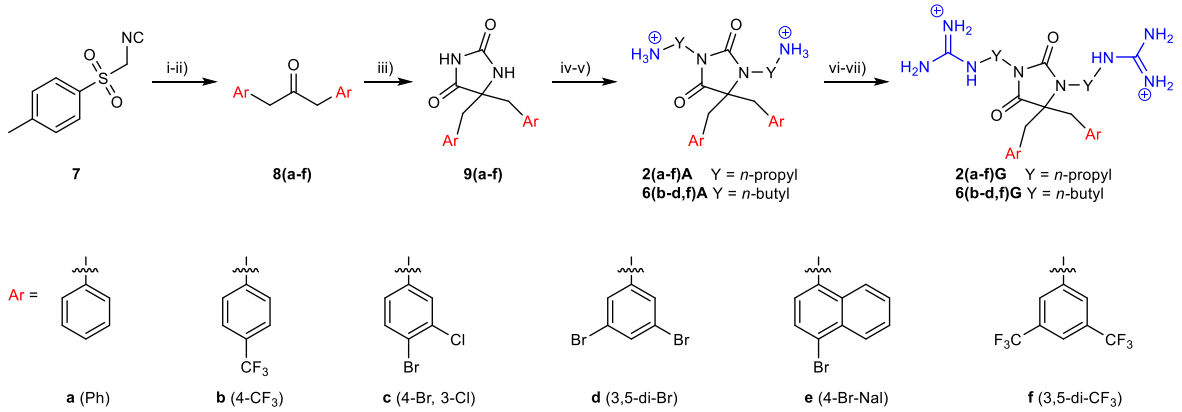

Scheme 1. Synthetic strategy towards target hydantoins **2** and **6**. Reaction conditions: i) $ArCH_2Br$, TBAB or TBAI, DCM, $NaOH_{(aq)}$ (20–35 wt%), r.t.; ii) $HCl_{(conc)}$, DCM/THF, r.t., 53–69% o2s; iii) KCN, NH_4CO_3, KOAc, DMSO or KCN, NH_4CO_3, EtOH/H_2O, 60–75 °C, 45–85%; iv) *N*-Boc-3-bromopropylamine or *N*-Boc-4-bromobutylamine, Cs_2CO_3, TBAI, acetone, 65 °C *then* v) TFA, DCM, r.t., 45–85% o2s; vi) *N,N′*-Di-Boc-1*H*-pyrazole-1-carboxamidine, DIPEA, THF, 45 °C *then* vii) TFA, DCM, r.t., 33–91% o2s.

diphenylpropan-2-one (Ar = Ph) could be prepared following this protocol. The other derivatives proved to be insoluble and the solvent needed to be changed to DMSO. Interestingly, an additional base, potassium acetate, was needed to obtain the hydantoins **9(a–f)** in moderate to high yields of 45–85%. For *N,N′*-dialkylation, the hydantoins **9(a–f)** were treated with *N*-Boc-3-bromopropylamine or *N*-Boc-4-bromobutylamine, caesium carbonate (Cs_2CO_3) and tetrabutylammonium iodide (TBAI) in acetone at elevated temperature.

Subsequent TFA/DCM induced Boc removal delivered the target hydantoins **2A** and **6A** in 45–85% over two steps. Conversion of the amine-modified hydantoins **2A** and **6A** to their guanidyl counterparts was achieved with *N,N′*-di-Boc-1*H*-pyrazole-1-carboxamidine and *N,N*-diisopropylethylamine (DIPEA) in THF. Ensuing Boc removal with TFA/DCM delivered guanidyl hydantoins **2G** and **6G** in 33–91% yield o2s.

2.2.2. *4-Imidazolidin-2-one **3A** and 2-(hydroxy)-1H-imidazole **15A***

We first set out to obtain the 4-imidazolidin-2-one derivative **3A** by a two-step process from the Boc protected hydantoin **2dA** (Ar = 3,5-diBrPh) (see Supporting Information, Scheme S1 and Table S1). Even though the transformation was feasible, **3A** could not be purified satisfyingly. Therefore, we changed the synthetic strategy as shown in Scheme 2. Starting from 3,5-dibromobenzaldehyde **10**, we employed a Wittig reaction with $Ph_3PCH_2(OMe)Cl$ to generate the corresponding vinyl ether in 91% yield as a 1.5:1.0 mixture of the *E*- and *Z*-isomer as by ^1H NMR. Treatment of the vinyl ether with hydrochloric acid in THF and formic acid or TFA in DCM resulted in complex mixtures. Using *in-situ* generated HCl by combining oxalyl chloride, EtOH and H_2O [48] led to quick and full conversion to the desired aldehyde, but the results were not always reproducible. The most reliable results were finally achieved by using trimethylsilyl chloride (TMS-Cl) and sodium iodide in dry MeCN with high dilution [49]. The homologated aldehyde **11** was obtained in 60% yield. Aldehyde **11** was subsequently converted in a benzoin-type condensation to the α-hydroxy ketone **12** by treatment with Et_3N and catalytic amounts of 3-benzyl-5-(2-hydroxyethyl)-4-methylthiazolium chloride in dry PEG-400 [50]. We used PEG-400 instead of the more commonly employed EtOH [50], due to the low solubility of aldehyde **11**. Based on literature [51], we condensed the α-hydroxy ketone **12** with urea in the presence of glacial acetic acid in anhydrous PEG-400. We obtained 4-imidazolin-2-one **14** in 39% yield as the major product and found unexpectedly 4-oxazolin-2-one **13** in 18% yield. In previous reports, the side product was only observed when the benzoin reagent had electron donating substituents (4,4′-dimethoxybenzoin) or heterocyclic nitrogen (2,2′-pyridoin) [51]. The authors were reasoning that the electron donating *para*-methoxy substituents would render the hydroxyl group of the intermediate more nucleophilic as does the basic pyridinyl nitrogen by intramolecular hydrogen bonding. One possible explanation could be the bromine atom acting as a Lewis base, forming a hydrogen bond to the hydroxyl hydrogen. This interaction would be comparable to the basic pyridinyl hydrogen and would facilitate an intramolecular attack of the urea oxygen, leading to compound **13**.

We then alkylated 4-oxazolin-2-one **13** and 4-imidazolidin-2-one **14**, respectively, with *N*-boc-3-bromopropylamine using (*n*-hexadecyl)tri-*n*-butylphosphonium bromide as phase transfer catalyst and potassium carbonate as a base in a biphasic mixture of water and toluene under μ-wave irradiation. Subsequently, the di-alkylated products were

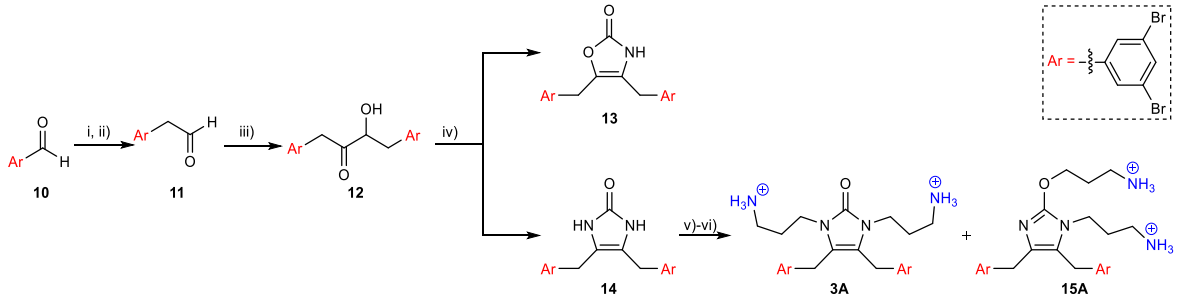

Scheme 2. Synthetic strategy towards tetrasubstituted 4-imidazolidin-2-one **3A** and its constitutional isomer **15A.** Ar = 3,5-dibromophenyl. Reaction conditions: i) $Ph_3PCH_2(OMe)Cl$, NaHMDS, THF (dry), −78 °C to r.t., 91%; *E/Z* = 1.5/1.0; ii) TMSCl, NaI, MeCN (dry), r.t., 60%; iii) 3-benzyl-5-(2-hydroxyethyl)-4-methylthiazolium chloride, Et_3N, PEG-400 (dry), 80 °C, 39%; iv) urea, AcOH, PEG-400 (dry), 130 °C, 18% for **13** and 39% for **14**; v) *N*-Boc-3-bromopropylamine, K_2CO_3, (*n*-hexadecyl)tri-*n*-butylphosphonium bromide, toluene:water, μ-wave, 130–150 °C *then* vi) TFA, DCM, r.t., 17–19% o2s.

deprotected with TFA/DCM. Synthesis of the derivative from 4-oxazolin-2-one **13** delivered a di-alkylated compound with an unresolved structure and was not further investigated.

Compound **14** delivered the desired *N,N′*-dialkylated 4-imidazolin-2-one **3A** in low yields (19% o2s). Surprisingly, *N,O*-dialkylated 2-(hydroxy)-1*H*-imidazole **15A** (17% o2s) was obtained from the same reaction mixture. The mono alkylated derivatives of structures **3A** and **15A** were obtained as well, partially explaining the low yields.

2.2.3. 2,4-Dithiohydantoin *4A*

By employing *in situ* generated NH_4CN and CS_2 [52] we intended to obtain 2,4-thiohydantoin **4A** from ketone **8d** (Ar = 3,5-di-BrPh), but no conversion was observed. Instead hydantoin **9d** (3,5-di-Br) was treated with the Lawesson's reagent at elevated temperature [53] to deliver 2, 4-thiohydantoin **16** (3,5-di-Br) in 82% yield (Scheme 3). *N, N′*-Dialkylation of **16** with *N*-Boc-3-bromopropylamine afforded 2, 4-dithiohydantoin **4A** in 56% yield.

2.2.4. 2-Thiobarbituric acid *5A*

In a first approach we tried to thiolate 5,5-bis(3,5-dibromobenzyl) barbituric acid with the Lawesson's reagent under the same conditions as used to obtained 2,4-dithiohydantoins (*vide supra*). Unfortunately, we obtained an inseparable mixture of the mono-, di- and tri-thiolated barbituric acid. Therefore, we decided to adapt our previously reported procedure [17] by replacing urea with thiourea. Treatment of di-benzylated diethyl malonate **17** and thiourea with NaH in a mixture of anhydrous THF and DMF gave the 5,5-dibenzylated-2-thiobarbituric acid **18** in low yields (Scheme 4). *N*-alkylation with *N*-Boc-3--bromopropylamine, Cs_2CO_3 and TBAI in acetone at elevated temperature, followed by TFA/DCM mediated Boc removal delivered the tetrasubstituted barbiturates **5A** and **1A** in very low yields (9%). Partial desulfurization had taken place, resulting in two mixtures of tetrasubstituted 2-thiobarbituric acid **5A** (X = S) and barbituric acid **1A** (X = O). Mixture 1 constituted a ratio of 2.4:1.0 (**5A:1A**) and mixture 2 constituted a ratio of 1.0:1.7 (**5A:1A**). The mixtures were inseparable but stable in solid state and were tested as such. Only when the mixtures were in solution, we could see slow desulfurization take place, potentially by low amounts of peroxide formation from atmospheric oxygen under light exposure [54,55].

2.3. SAR analysis

All compounds were screened for their antimicrobial activity against antibiotic susceptible Gram-positive and Gram-negative bacterial reference strains. Antimicrobial potency of each compound was expressed by their minimum inhibitory concentration (MIC) values. Haemolytic activity against human red blood cells (RBC), expressed by the EC_{50} value, was used as a measurement of cytotoxicity. The ideal compound should display high bacterial activity (low MIC values) and low or no toxicity towards human cells (high EC_{50} values) i.e. acting

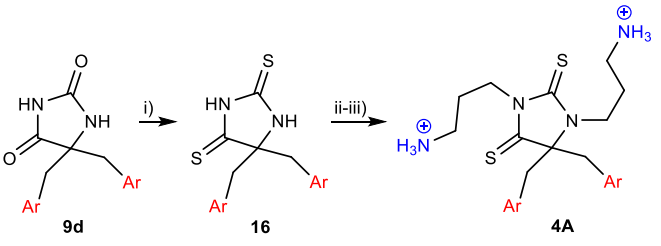

Scheme 3. Synthetic strategy towards 2,4-dithiohydantoin **4A**. Ar = 3,5-dibromophenyl. Reaction conditions: i) Lawesson's reagent, 1,4-dioxane, 115 °C, 82%; ii) *N*-Boc-3-bromopropylamine, Cs_2CO_3, TBAI, acetone, 55 °C then iii) TFA, DCM, r.t., 56%.

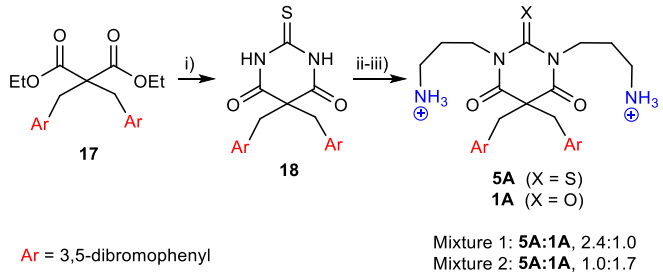

Scheme 4. Synthetic strategy towards 2-thiobarbituric acid **5A**. Mixtures of 2-thiobarbituric acid **5A** (X = S) and barbituric acid **1A** (X = O) were obtained. Ar = 3,5-dibromophenyl. Reaction conditions: i) Thiourea, NaH, anhydrous THF:DMF, 65 °C, 24%; ii) *tert*-butyl (3-bromopropyl)carbamate, Cs_2CO_3, TBAI, acetone, 70 °C, then iii) TFA, DCM, r.t., 9% o2s.

selectively against bacteria. As a reference compound we used the already reported barbiturate **1A** [20] (Table 1, entry 7). The commercially available antibiotic ciprofloxacin served as a positive control (entry 8). Capital **A** in the compound codes denotes cationic amine derivatives and capital **G** denotes cationic guanidine derivatives. For Series 2 and 3 the substituents on the phenyl groups are given in brackets for each compound to aid the discussion. The hydrophilicity of each core structure, bearing four substituents, was calculated using the ChemBioDraw Ultra software (PerkinElmer, v19.0.0.1.28).

2.3.1. Exploring new scaffolds

We started our investigation by comparing the different scaffolds **2dA**, **3A**, **4A**, **5A** and **15A** to identify the most promising candidate in terms of antimicrobial and haemolytic activity (Table 1). All scaffolds were decorated with the same lipophilic (Ar = 3,5-dibromophenyl) and cationic group (R^1 = 3-aminoprop-1-yl). The five membered hydantoin **2dA** (entry 1) was marginally less potent (MIC: 4–16 μg/mL) than the

Table 1
Antimicrobial activity (MIC in μg/mL) against bacterial reference strains and haemolytic activity against human RBC (EC_{50} in μg/mL) for compounds with different scaffold structures.

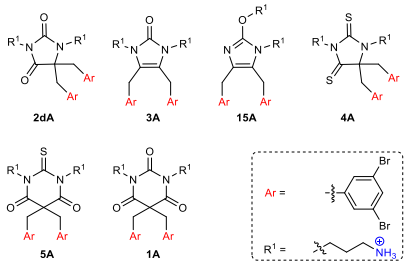

Entry	Comp. ID	CLogP[a]	Antimicrobial activity				EC_{50}
			S. a	B. s	E. c	P. a	
1	**2dA**	−1.69	8	4	16	8	344
2	**3A**	−0.47	2	1	4	8	52
3	**15A**	0.26	2	2	4	4	44
4	**4A**	−1.22	8	8	16	32	385
5	Mixture 1[b]	n.d.	8	4	8	16	305
6	Mixture 2[c]	n.d.	8	4	8	8	182
7 [20]	**1A**	−1.44	4	4	8	8	99
8	Ciprofloxacin		0.06	<0.03	<0.03	0.25	

Bacterial reference strains: S. a – *Staphylococcus aureus* ATCC 9144, B. s – *Bacillus subtilis* 168, E. c – *Escherichia coli* ATCC 25922, and P. a – *Pseudomonas aeruginosa* ATCC 27853.

[a] ClogP values were calculated for the respective tetrasubstituted core structures (calculated with ChemBioDraw Ultra). n.d.: not determined.

[b] Mixture of 2.4:1.0 (**5A:1A**).

[c] Mixture of 1.0:1.7 (**5A:1A**).

barbituric acid **1A** (entry 7), although it was estimated to be slightly more hydrophilic. Interestingly, hydantoin **2dA** was almost 3.5 times less haemolytic (EC_{50}: 344 μg/mL) than **1A** (EC_{50}: 99 μg/mL). The 4-imidazolidin-2-one core **3A** (entry 2) was one order of magnitude more lipophilic than the hydantoin core. **3A** demonstrated a 4-fold increase in antimicrobial potency (MIC: 1–4 μg/mL) against all strains except for the Gram-negative bacterium *Pseudomonas aeruginosa*, but also a 7-8-fold increase in haemolytic activity (EC_{50}: 52 μg/mL). The constitutional isomer 4-oxazolin-2-one **15A** (entry 3) gave a similar result (MIC: 2–4 μg/mL, EC_{50}: 44 μg/mL). Despite being very potent, the systemic application of these compounds is limited by their high haemolytic activity.

It did not become clear why these core structures were so distinctively more haemolytic than hydantoin **2dA**. The 2,4-dithiohydantion **4A** (entry 4) displayed a 4-fold decrease in activity against *P. aeruginosa* (MIC: 32 μg/mL) compared to its dioxo counterpart **2dA**. The dithio-derivative **4A** was only marginally less haemolytic (EC_{50}: 385 μg/mL) than **2dA** (EC_{50}: 344 μg/mL).

Mixture 1 (entry 5), being enriched with 2-thiobarbituric acid **5A** (ClogP = −0.52), exhibited reduced potency against the Gram-negative *P. aeruginosa* (MIC: 16 μg/mL) and the haemolytic activity (EC_{50}: 305 μg/mL) was decreased by a factor of three compared to **1A** (EC_{50} = 99 μg/mL). By reduction of the amount of **5A** in mixture 2 (entry 6), antimicrobial activity (MIC: 4–8 μg/mL) and more pronouncedly the haemolytic activity (EC_{50}: 182 μg/mL) approached the values found for **1A** (entry 7). In conclusion, the sulphur containing derivatives were less haemolytic and less potent against the Gram-negative *P. aeruginosa*. No major change in activity was observed against the other bacterial test strains. Combined with the synthetic challenges and the chemical instability, thionylated derivatives were not worthwhile to investigate further. Clearly the hydantoin scaffold was the most promising core structure for further development.

2.3.2. Hydantoins with n-propyl linkers (2)

A series of hydantoins **2** (Table 2) with *n*-propyl linkers connecting the cationic amino (**A**) or guanidino (**G**) groups to the core were constructed to screen additional lipophilic side chains (**a-c** and **e-f**) for their impact on the compounds' potency and haemolytic toxicity. We have chosen (pseudo)halogenated benzyl groups as lipophilic side chains based on their potential influence on the antimicrobial potency and haemolytic activity described in previous studies [16,17,20]. The trends observed in this study were similar to previous studies and will not be repeated in detail here. The compounds are ranged according to increasing lipophilicity.

Generally, the compounds in amine series **2(a-f)A** (Table 2, entry 1–6) exhibited improved antibacterial potency and increased haemolytic activity with higher CLogP values of the lipophilic side chains, except for hydantoin **2 fA** (3,5-di-CF_3). Derivatives **2aA** (Ph) and **2bA** (4-CF_3) were practically inactive against all strains (MIC: 16–>256 μg/mL). Amine hydantoin **2cA** (4-Br, 3-Cl) was only active against the Gram-positive strains, *Bacillus subtilis* and *Staphylococcus aureus* (MIC: 4–8 μg/mL), whereas the amine hydantoins **2(d-f)A** (entries 4–6) were

Table 2
Antimicrobial activity (MIC in μg/mL) against bacterial reference strains and haemolytic activity against human RBC (EC_{50} in μg/mL) for tetrasubstituted hydantoins **2** and **6**.

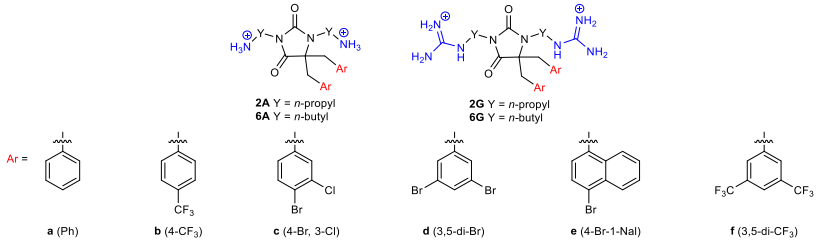

Entry	Comp. ID	Ar	Y	CLogP[a]	Antimicrobial activity				EC_{50}[b]
					S. a	B. s	E. c	P. a	
1	**2aA**	(Ph)	*n*-propyl	2.64	>256	256	>256	>256	>311
2	**2bA**	(4-CF_3)	*n*-propyl	3.52	64	16	256	>256	>379
3	**2cA**	(4-Br, 3-Cl)	*n*-propyl	4.08	8	4	32	32	368
4	**2dA**	(3,5-di-Br)	*n*-propyl	4.38	8	4	16	8	344
5	**2eA**	(4-Br-1-Nal)	*n*-propyl	4.68	4	4	8	8	69
6	**2fA**	(3,5-di-CF_3)	*n*-propyl	5.03	16	8	16	16	399
7	**2aG**	(Ph)	*n*-propyl	2.64	64	128	>256	>256	>353
8	**2bG**	(4-CF_3)	*n*-propyl	3.52	16	8	128	>256	>421
9	**2cG**	(4-Br, 3-Cl)	*n*-propyl	4.08	2	2	32	64	>467
10	**2dG**	(3,5-di-Br)	*n*-propyl	4.38	2	4	16	32	486
11	**2eG**	(4-Br-1-Nal)	*n*-propyl	4.68	2	2	8	32	206
12	**2fG**	(3,5-di-CF_3)	*n*-propyl	5.03	4	2	32	32	>489
13	**6bA**	(4-CF_3)	*n*-butyl	3.52	64	16	>128	>128	>393
14	**6cA**	(4-Br, 3-Cl)	*n*-butyl	4.08	8	4	64	64	>439
15	**6dA**	(3,5-di-Br)	*n*-butyl	4.38	8	2	32	32	364
16	**6fA**	(3,5-di-CF_3)	*n*-butyl	5.03	16	4	64	64	>461
17	**6bG**	(4-CF_3)	*n*-butyl	3.52	4	4	64	>128	>503
18	**6cG**	(4-Br, 3-Cl)	*n*-butyl	4.08	1	1	8	32	347
19	**6dG**	(3,5-di-Br)	*n*-butyl	4.38	1	1	4	16	206
20	**6fG**	(3,5-di-CF_3)	*n*-butyl	5.03	2	2	8	32	384
21	Ciprofloxacin				0.06	<0.03	<0.03	0.25	

Bacterial reference strains: S. a – *Staphylococcus aureus* ATCC 9144, B. s – *Bacillus subtilis* 168, E. c – *Escherichia coli* ATCC 25922, and P. a – *Pseudomonas aeruginosa* ATCC 27853.

[a] ClogP values were calculated for substituted benzyl groups (calculated with ChemBioDraw Ultra).

[b] Values given as *greater than* correspond to the highest concentration (500 μM) tested in the RBC assay.

potent against all strains tested (MIC: 4–16 μg/mL). The most potent amine derivative was **2eA** (4-Br-1-Nal), showing good broad-spectrum potency (MIC: 4–8 μg/mL). Interestingly, it was at least 5-times more haemolytic (EC_{50}: 69 μg/mL) than any of the other amine derivatives (**2A**). Hydantoin **2fA** (3,5-di-CF_3) was more lipophilic than **2eA** (4-Br-1-Nal) but less potent (MIC: 8–16 μg/mL) than the latter by a factor of two to four. The electron withdrawing trifluoromethyl groups may lead to a slight polarisation of the aromatic ring, thus reducing its ability to interact with the lipid membrane. The most promising amine derivative was **2dA** (3,5-di-Br), having broad-spectrum activity (MIC: 4–16 μg/mL) and negligible haemolytic activity (EC_{50}: 344 μg/mL). Surprisingly, it demonstrated slightly higher activity against *P. aeruginosa* than *Escherichia coli*

The guanidyl series **2(a-f)G** (Table 2, entry 7–12) exhibited the same general trend for antimicrobial potency and haemolytic activity as in the amine series, except for derivative **2fG** (3,5-di-CF_3). The guanidyl derivatives were generally more potent against the Gram-positive strains than their amine counterparts by a factor of two to four. Guanidyl hydantoins **2(b-f)G** (entries 8–12) exhibited good to very good potency (MIC: 2–16 μg/mL) against the Gram-positive strains. The potency against the Gram-negative *E. coli* was virtually unchanged compared to their amine correlates. However, the activity against the Gram-negative *P. aeruginosa* decreased two-fold for **2cG** (4-Br, 3-Cl) and **2fG** (3,5-di-CF_3), and four-fold for **2dG** (3,5-di-Br) and **2eG** (4-Br-1-Nal), correspondingly. All guanidyl derivatives were pronouncedly less haemolytic than their amine equivalents. The most promising guanidine derivative was **2eG** (4-Br-1-Nal), which demonstrated good potency against all bacterial strains (MIC: 2–8 μg/mL) except for *P. aeruginosa* and had low haemolytic toxicity (EC_{50}: 206 μg/mL). The combination of *n*-propyl linkers and guanidyl head groups having improved potency against Gram-positive strains and reduced potency against the Gram-negative *P. aeruginosa*, as well as reduced haemolytic activity, has also been observed for amphipathic barbiturates [20].

In summary, guanidyl derivatives **2(c-f)G** showed good potency against both Gram-positive test strains (MIC: 2–4 μg/mL), but none of the guanidyl derivatives **2G** were potent against *P. aeruginosa*. Amines **2dA** (3,5-di-Br) and **2eA** (4-Br-1-Nal) were the most potent derivatives of hydantoins **2**, with **2dA** (3,5-di-Br) being non haemolytic.

2.3.3. Hydantoins with n-butyl linkers (6)

In our previous study on tetrasubstituted barbiturates, a combination of guanidyl head groups and *n*-butyl linkers achieved the highest broad-spectrum activity. Due to the structural similarity, we reasoned that *n*-butyl linkers would boost the hydantoins' potency. We chose the most promising side chains **b** (4-CF_3), **c** (4-Br, 3-Cl), **d** (3,5-di-Br) and **f** (3,5-di-CF_3) from hydantoin derivatives **2**.

Amine hydantoins **6A** displayed the same potency against the Gram-positive strains as derivatives **2A** but had reduced activity against the Gram-negative strains by a factor of two to four (Table 2). None of the derivatives were haemolytic (EC_{50}: ≥364 μg/mL).

Upon guanylation, all compounds of **6G** became highly potent against the Gram-positive strains (MIC: 1–4 μg/mL). Guanidino hydantoin **6cG** (4-Br, 3-Cl) demonstrated good activity against all strains (MIC: 1–8 μg/mL), except for *P. aeruginosa*, with no noteworthy haemolytic activity (EC_{50}: 347 μg/mL). Hydantoin **6dG** (3,5-di-Br) had excellent activity against the Gram-positive strains (MIC: 1 μg/mL) and good to moderate activity against the Gram-negative strains (MIC: 4–16 μg/mL).

In summary, we did observe increased potency and haemolytic activity for the guanidyl compounds **6G** compared to their amine counterparts **6A** (*vide supra*). While being non-haemolytic, the potency of the amine derivatives was rather unsatisfying. The guanidyl compounds **6cG** (4-Br, 3-Cl) and **6dG** (3,5-di-Br), however, displayed promising antimicrobial potency and low to no haemolytic activity.

2.4. Selectivity index and counterion effect

The selectivity index (SI) is a simple descriptor given by the ratio of EC_{50}/MIC for the efficiency of antimicrobial agents. We have summarized the most promising compounds with their SI values in Table 3. Compounds were only considered active if the MIC value was ≤16 μg/mL. SI values for all other compounds can by found in the Supporting Information, Table S3.

Compounds **2cG** (4-Br, 3-Cl), **2fG** (3,5-di-CF_3), **6cA** (4-Br, 3-Cl) **2dG** (3,5-di-Br), **2eG** (4-Br-1-Nal), **6cG** (4-Br, 3-Cl) and **6fG** (3,5-di-CF_3) demonstrated excellent selectivity for the Gram-positive strains (entries 1–7). Hydantoins **2dG**, **2eG, 6cG** and **6fG** (entries 4–7) had additionally good selectivity (SI: >20) for *E. coli*. All seven derivatives showed low to no haemolytic toxicity. Derivatives **2dA** (3,5-di-Br), **2fA** (3,5-di-CF_3) and **6dG** (3,5-di-Br) had good SI values for all strains tested (entries 8–10). The hydantoins **2dA** (3,5-di-Br) and **2fA** (3,5-di-CF_3) had SI values >20 against the Gram-negative bacterium *P. aeruginosa*, while **6dG** (3,5-di-Br) had SI: 13 for *P. aeruginosa*. All these can be considered very promising compounds.

All compounds tested were obtained as di-trifluoroacetate (di-TFA) salts, which are non-physiological. Therefore, we converted **2cA**, **2cG**, **2dA** and **2dG** to physiological di-hydrochloride (di-HCl) salts, to assess if the biological behaviour would be altered (see Supporting Information, Table S2). We did not observe any major changes in the MIC or EC_{50} values for any of these four derivatives. Minor improvements in antimicrobial activity could be observed for the di-HCl salts of **2cA** (4-Br, 3-Cl) and **2cG** (4-Br, 3-Cl), but no clear trend was apparent. Also, the haemolytic activity was only influenced to a small extend and could often be correlated to the lower molecular weight of the di-HCl salts compared to the di-TFA salts.

2.5. Mode of action (MoA) studies

We have examined the effects of the compounds on the viability of bacterial cells and the membrane integrity of bacterial cells. Seven compounds were selected (based on structural alterations, MIC values, haemolytic activity, and SI) for MoA studies against *B. subtilis* 168 (see Supporting Information, Table S4), as they were primarily potent against Gram-positive bacteria. Six additional compounds with broad-spectrum activity were selected for MoA studies against both, *B. subtilis* 168 and *E. coli* K12 (see Supporting Information, Tables S4 and S5) [56]. These two well-known strains of *B. subtilis* and *E. coli*, in combination with the respective sensor plasmids that carry the reporter constructs, serve as models to study the modes of action in

Table 3
Selectivity index (SI) of the most promising narrow- and broad-spectrum antimicrobials. EC_{50} values are given in [μg/mL].

Entry	Comp. ID	SI (EC_{50}/MIC)[a]				EC_{50}[b]
		S. a	B. s	E. c	P. a	
1	**2cG**	>234	>234	–	–	>467
2	**2fG**	>122	>245	–	–	>489
3	**6cA**	>55	>110	–	–	>439
4	**2dG**	243	122	30	–	486
5	**2eG**	103	103	26	–	206
6	**6cG**	347	347	43	–	347
7	**6fG**	192	192	48	–	384
8	**2dA**	43	86	22	43	344
9	**2fA**	25	50	25	25	399
10	**6dG**	206	206	52	13	206

Bacterial reference strains: S. a – *Staphylococcus aureus* ATCC 9144, B. s – *Bacillus subtilis* 168, E. c – *Escherichia coli* ATCC 25922, and P. a – *Pseudomonas aeruginosa* ATCC 27853.

[a] –: No SI was calculated if MIC was >16 μg/mL.

[b] Values given as *greater than* correspond to the highest concentration (500 μM) tested in the RBC assay.

representatives of Gram-positive and Gram-negative bacteria, respectively.

To explore the MoA of promising compounds in *B. subtilis* 168 and *E. coli* K12, we conducted two luciferase-based biosensor tests – examining the effects on bacterial viability and membrane integrity. The biosensor-based viability test measures the viability of bacterial cells as light production by recombinantly expressed bacterial luciferase derived from the *Photorhabdus luminescens lux* operon [57,58]. External substrates do not affect light production by bacterial lux operons. Bacteria themselves provide a reduced flavin mononucleotide (FMNH2) and a long-chain aldehyde pool, which is the substrate for light production. Bacterial luciferase is a very efficient real-time sensor of bacterial viability because NADH, NADPH, and ATP are required to constantly fill the substrate pool.

The biosensor-based membrane integrity test is based on the *luc*GR gene (luciferase) of *Pyrophorus plagiophthalamus*, which is a luminous click beetle [59]. Unlike bacterial luciferase, the light reaction is closely dependent on externally added D-luciferin as a substrate. D-luciferin cannot cross the intact biological membrane properly at neutral pH. The uptake of D-luciferin is explored after the addition of antimicrobial substances to determine whether the membrane has been affected and becomes permeable for D-luciferin or not. If D-luciferin enters through damaged membranes, light production increases. Light production peaks quickly if the integrity of the membrane is compromised and then usually decreases during the consumption of the dying cells' ATP.

In general, most of the compounds tested influenced survival (viability) and showed strong membrane disrupting activity against *B. subtilis*, and some of them were active against both bacterial species. However, some compounds had more prominent effects on survival and faster membranolytic effects on *B. subtilis* than *E. coli*. When the concentration of the compounds exceeded the MIC value against the respective bacterium, both the viability and the integrity of the membrane were affected for most compounds. Furthermore, increasing concentrations affected both viability and membranolytic activity at an increasing rate, indicating a concentration-dependent killing effect. However, we were unable to determine the relationship between the structure/activity and the mode of action profiles. Compound **6cG** (4-Br, 3-Cl) was chosen as a broad-spectrum hydantoin to illustrate the results with regard to viability and membrane integrity (Figs. 3 and 4). During the 3 min test period, hydantoin **6cG** showed a substantial influence on the survival (viability) of *B. subtilis* (Fig. 3A, left). The derivative **6cG** showed a membrane-related action because the light emittance increased rapidly and dose-dependently (Fig. 3B, left), and the effect was prominent compared to chlorhexidine (CHX) (Fig. 3B, right). The CHX reference control is a bactericidal agent that affects the cell walls and membranes of both *B. subtilis* 168 [60] and *E. coli* K12 [61]. In the present study, the MIC value for CHX was determined to be 1.5 μg/mL against both *B. subtilis* 168 and *E. coli* K12. The disruptive membrane effect of hydantoin **6cG** on *B. subtilis* was shown to occur at a concentration of 25.6 and 51.2 μg/mL (blue and black line, Fig. 3B, left), which were 25.6 and 51.2 times higher than its MIC (1 μg/mL). Concentrations below 25.6 μg/mL showed a limited membrane disruption effect, with peak emissions not decreasing during the measurement period. The bacterial concentration in these experiments was approximately 100 times higher than that used in the MIC test, and this could explain why a higher concentration of **6cG** hydantoin was required to affect the viability and integrity of the membrane.

The effect of hydantoin **6cG** on the viability and membrane integrity of the Gram-negative *E. coli* showed somewhat incomparable effects as observed towards the Gram-positive *B. subtilis*. Being a broad-spectrum derivative, **6cG** could not influence the viability of *E. coli* as fast as the strong membranolytic agent CHX (Fig. 4A). Although a concentration-dependent declining trend of light emission was seen in the viability assay, only the highest concentration (51.2 μg/mL which is 6.4 x MIC) resulted in increased light emission in the inner membrane assay and it was not followed by a decline during the test period (indicating a less notable disruptive effect of the inner membrane) (Fig. 4B, left). The delay and reduction in the effect of **6cG** on membrane integrity could be caused by the outer membrane of *E. coli,* which may act as an additional barrier.

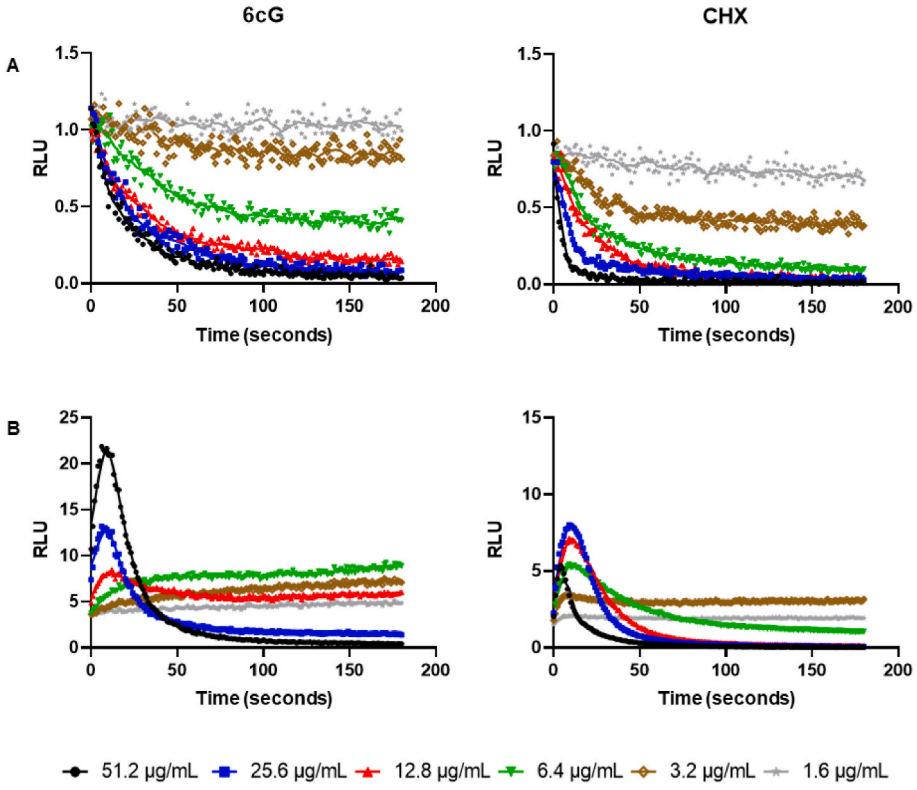

Fig. 3. The effects of **6cG** (broad spectrum) and chlorhexidine (CHX, positive control) on the kinetics of (**A**) viability and (**B**) membrane integrity in *B. subtilis* 168. Normalized light emission (normalized with a negative, untreated water control) is plotted as relative light units (RLU) over time (seconds). Light emission was measured each second for 180 s after adding the bacterial cell suspension (with 1 mM D-luciferin for the membrane integrity assay) to the analytes in separate wells. The figure shows a representative data set from at least three independent experiments.

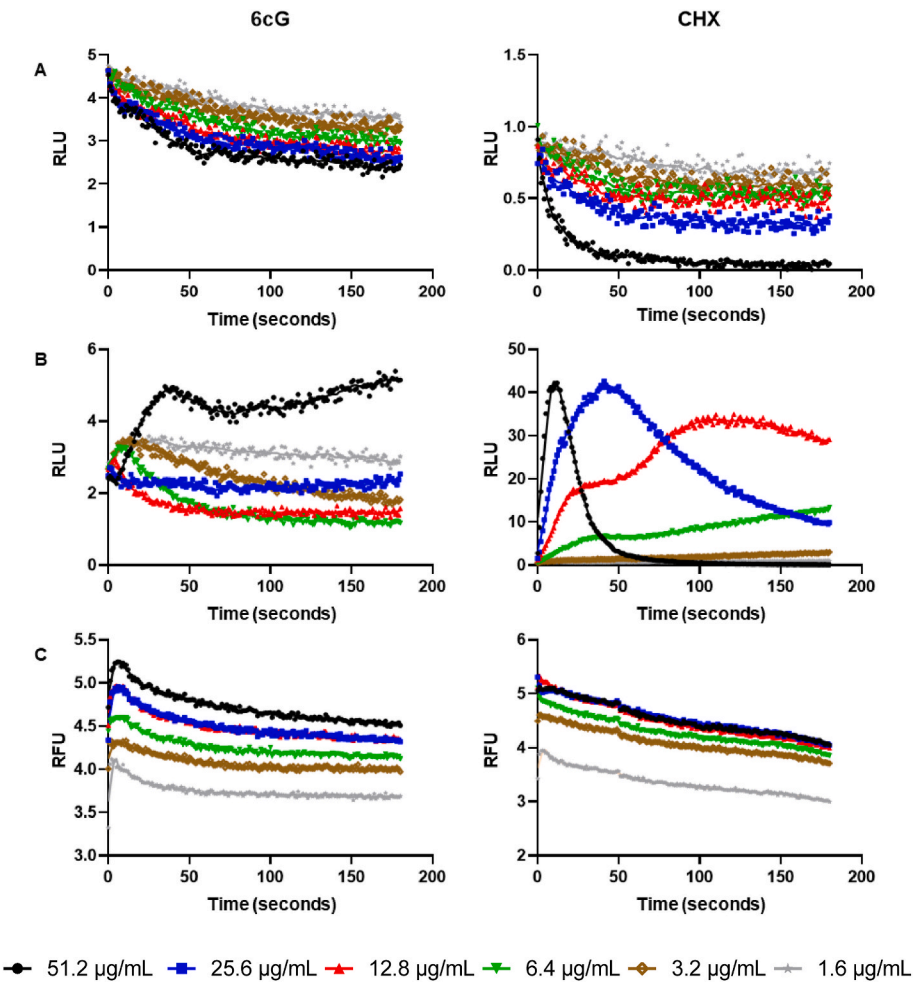

Fig. 4. The effects of **6cG** (broad spectrum) and chlorhexidine (CHX, positive control) on the kinetics of (A) viability, (B) inner membrane integrity, and (C) outer membrane integrity in *E. coli* K12. Normalized light emission (normalized with a negative, untreated water control) is plotted as relative light units (RLU) over time (seconds) for A and B. For C, normalized fluorescence (normalized with a negative, untreated water control) is plotted as relative fluorescence units (RFU) over time (seconds). Light emission/fluorescence was measured each second for 180 s after adding the bacterial cell suspension (with 1 mM D-luciferin for the inner membrane integrity assay and 20 µM 1-*N*-phenylnapthylamine for outer membrane integrity assay) to the analytes in separate wells. The figure shows a representative data set from at least three independent experiments.

We used the 1-*N*-phenylnapthylamine (NPN) fluorescent probe to determine whether **6cG** affected the outer membrane permeability of *E. coli*. The small NPN molecules (219 Da) have low fluorescence in water solutions, but if bound to phospholipids, they produce high fluorescence. Hydrophobic NPN cannot effectively pass through the outer membrane of intact *E. coli* cells, resulting in low fluorescence; however, if the outer membrane is damaged, NPN can reach the periplasmic space, bind to the phospholipids of the inner and outer membrane, and produce enhanced fluorescence [62]. In this test, high concentrations of hydantoin **6cG** produced high fluorescence levels (Fig. 4C, left), while no significant increase in luminescence was observed in the inner membrane integrity test, except in one concentration which is 51.2 µg/mL (Fig. 4B, left). This observation indicates that the presence of the outer membrane may be a rate-limiting step for this compound to act on the inner membrane. However, when the concentration of **6cG** increased, the fluorescence level was higher (Fig. 4C, left), indicating a rapid change in outer membrane permeability that was followed by membrane disruption as compared to CHX (Fig. 4C, right). At the same time, bacterial cell survival was reduced (Fig. 4A, left) and the integrity of the inner membrane was altered (Fig. 4B, left).

The viability of the bacterial cells was markedly reduced for a concentration of 51.2 µg/mL (6.4 x MIC) (see Fig. S1), and when samples from the NPN assay were spotted on an agar plate after the test period, a bactericidal effect of **6cG** was demonstrated. These results strongly suggest that when concentrations are high enough, hydantoin **6cG** disrupts the outer and inner membranes at the same speed. However, it cannot be excluded that higher concentrations of **6cG** cause a different MoA, leading the compound to cross the outer membrane without affecting the latter.

Our results indicate that the main MoA of most of the synthesized compounds is to interrupt the integrity of the bacterial membranes in a concentration-dependent manner – as demonstrated for the broad-spectrum hydantoin **6cG,** against both the Gram-positive *B. subtilis* and the Gram-negative *E. coli*. However, some cationic AMPs have a concentration-dependent dual mode of action [63]. For example, it is known that the N-terminal fragment 1–35 of Bac7 (a proline-arginine rich AMP) has an effect on the internal membrane at high concentrations and binds to the intracellular chaperone protein DnaK and 70S ribosomes, and affect these target molecules at low concentrations [64–66]. Hence, other targets may exist in addition to the bacterial cytoplasmic membranes. Further studies are needed to determine whether there are other additional modes of action for these compounds.

3. Conclusion

We investigated five scaffolds for their suitability to develop novel tetrasubstituted, amphipathic SMAMP antimicrobials, revealing the hydantoin structure as a promising template for antibacterial drug lead development. By screening different combinations of lipophilic side chains, *n*-alkyl linkers and cationic groups we identified the tetrahalogenated compounds **2dA** (3,5-di-Br), **6cG** (4-Br, 3-Cl) and **6dG** (3,5-di-Br) as very promising lead structures. The results obtained from the viability and membrane integrity assays, suggested a rapid membranolytic effect, as demonstrated for hydantoin **6cG** in *B. subtilis* and *E. coli*. Interestingly, both the inner and the outer membrane in *E. coli*

seemed to be disrupted at a similar speed. We believe that our findings on the qualitative contribution of the scaffold structures can help the development of novel small molecule analogues of AMPs or SMAMPs.

4. Experimental section

For a detailed description of all chemical and biological experimental procedures, chemical analysis and further discussions see the Supporting Information. Additional raw data is available through the DataverseNO repository, link: https://doi.org/10.18710/A6AJN4.

Author contributions

M.K.L, A.B. and M.B.S. designed the compound library; M.K.L carried out all chemical experiments and analysis; A.R., H.D., H.-M.B., T.H. and K.S. determined the biological assays; A.R., H.D., T.A. performed the biological assays and M.K.L, A.R., H.D., H.-M.B., T.H., K.S., A.B. and M. B.S. analysed and interpreted the data. The manuscript was written through contributions of all authors. All authors have given approval to the final version of the manuscript.

Declaration of competing interest

The authors declare the following financial interests/personal relationships which may be considered as potential competing interests: Morten B Strøm and Annette Bayer have patent #Barbituric acid derivatives comprising cationic and lipophilic groups. WO2018178198A1. Issued to UiT.

Data availability

NMR data files are available at DataverseNO: https://doi.org/10.18710/A6AJN4.

Acknowledgements

MKL, AR and HD thank for a PhD fellowship provided by UiT as part of the AntifoMar (2560700) and LeadScAMR (2017/6770) grants. We thank Senior Engineer Jostein Johansen for help with the HRMS and Prof. Máté Erdélyi for sharing his knowledge.

Appendix A. Supplementary data

Supplementary data to this article can be found online at https://doi.org/10.1016/j.ejmech.2023.115147.

References

[1] O. Nolte, Antimicrobial resistance in the 21st century: a multifaceted challenge, Protein Pept. Lett. 21 (2014) 330–335.
[2] M. Miethke, M. Pieroni, T. Weber, M. Brönstrup, P. Hammann, L. Halby, P. B. Arimondo, P. Glaser, B. Aigle, H.B. Bode, R. Moreira, Y. Li, A. Luzhetskyy, M. H. Medema, J.-L. Pernodet, M. Stadler, J.R. Tormo, O. Genilloud, A.W. Truman, K. J. Weissman, E. Takano, S. Sabatini, E. Stegmann, H. Brötz-Oesterhelt, W. Wohlleben, M. Seemann, M. Empting, A.K.H. Hirsch, B. Loretz, C.-M. Lehr, A. Titz, J. Herrmann, T. Jaeger, S. Alt, T. Hesterkamp, M. Winterhalter, A. Schiefer, K. Pfarr, A. Hoerauf, H. Graz, M. Graz, M. Lindvall, S. Ramurthy, A. Karlén, M. van Dongen, H. Petkovic, A. Keller, F. Peyrane, S. Donadio, L. Fraisse, L.J.V. Piddock, I. H. Gilbert, H.E. Moser, R. Müller, Towards the sustainable discovery and development of new antibiotics, Nat. Rev. Chem. 5 (2021) 726–749.
[3] M. Pasupuleti, A. Schmidtchen, M. Malmsten, Antimicrobial peptides: key components of the innate immune system, Crit. Rev. Biotechnol. 32 (2012) 143–171.
[4] C.D. Fjell, J.A. Hiss, R.E. Hancock, G. Schneider, Designing antimicrobial peptides: form follows function, Nat. Rev. Drug Discov. 11 (2011) 37–51.
[5] G. Carmona, A. Rodriguez, D. Juarez, G. Corzo, E. Villegas, Improved protease stability of the antimicrobial peptide Pin2 substituted with D-amino acids, Protein J. 32 (2013) 456–466.
[6] M. Su, D. Xia, P. Teng, A. Nimmagadda, C. Zhang, T. Odom, A. Cao, Y. Hu, J. Cai, Membrane-active hydantoin derivatives as antibiotic agents, J. Med. Chem. 60 (2017) 8456–8465.
[7] R. Kapoor, P.R. Eimerman, J.W. Hardy, J.D. Cirillo, C.H. Contag, A.E. Barron, Efficacy of antimicrobial peptoids against Mycobacterium tuberculosis, Antimicrob. Agents Chemother. 55 (2011) 3058–3062.
[8] C. Ghosh, G.B. Manjunath, P. Akkapeddi, V. Yarlagadda, J. Hoque, D.S. Uppu, M. M. Konai, J. Haldar, Small molecular antibacterial peptoid mimics: the simpler the better, J. Med. Chem. 57 (2014) 1428–1436.
[9] A. Violette, S. Fournel, K. Lamour, O. Chaloin, B. Frisch, J.P. Briand, H. Monteil, G. Guichard, Mimicking helical antibacterial peptides with nonpeptidic folding oligomers, Chem. Biol. 13 (2006) 531–538.
[10] P. Teng, Y. Shi, P. Sang, J. Cai, γ-AApeptides as a new class of peptidomimetics, Chem. Eur J. 22 (2016) 5458–5466.
[11] Y. Shi, P. Teng, P. Sang, F. She, L. Wei, J. Cai, γ-AApeptides: design, structure, and applications, Acc. Chem. Res. 49 (2016) 428–441.
[12] P. Teng, A. Nimmagadda, M. Su, Y. Hong, N. Shen, C. Li, L.-Y. Tsai, J. Cao, Q. Li, J. Cai, Novel bis-cyclic guanidines as potent membrane-active antibacterial agents with therapeutic potential, Chem. Commun. 53 (2017) 11948–11951.
[13] M. Wang, R. Gao, M. Zheng, P. Sang, C. Li, E. Zhang, Q. Li, J. Cai, Development of bis-cyclic imidazolidine-4-one derivatives as potent antibacterial agents, J. Med. Chem. 63 (2020) 15591–15602.
[14] M.B. Strøm, B.E. Haug, M.L. Skar, W. Stensen, T. Stiberg, J.S. Svendsen, The pharmacophore of short cationic antibacterial peptides, J. Med. Chem. 46 (2003) 1567–1570.
[15] T. Hansen, T. Alst, M. Havelkova, M.B. Strøm, Antimicrobial activity of small β-peptidomimetics based on the pharmacophore model of short cationic antimicrobial peptides, J. Med. Chem. 53 (2010) 595–606.
[16] M.H. Paulsen, D. Ausbacher, A. Bayer, M. Engqvist, T. Hansen, T. Haug, T. Anderssen, J.H. Andersen, J.U.E. Sollid, M.B. Strøm, Antimicrobial activity of amphipathic α,α-disubstituted β-amino amide derivatives against ESBL – CARBA producing multi-resistant bacteria; effect of halogenation, lipophilicity and cationic character, Eur. J. Med. Chem. 183 (2019), 111671.
[17] M.H. Paulsen, M. Engqvist, D. Ausbacher, T. Anderssen, M.K. Langer, T. Haug, G. R. Morello, L.E. Liikanen, H.-M. Blencke, J. Isaksson, E. Juskewitz, A. Bayer, M. B. Strøm, Amphipathic barbiturates as mimics of antimicrobial peptides and the marine natural products eusynstyelamides with activity against multi-resistant clinical isolates, J. Med. Chem. 64 (2021) 11395–11417.
[18] E.M. Igumnova, E. Mishchenko, T. Haug, H.-M. Blencke, J.U.E. Sollid, E.G. A. Fredheim, S. Lauksund, K. Stensvåg, M.B. Strøm, Synthesis and antimicrobial activity of small cationic amphipathic aminobenzamide marine natural product mimics and evaluation of relevance against clinical isolates including ESBL–CARBA producing multi-resistant bacteria, Biorg. Med. Chem. 24 (2016) 5884–5894.
[19] T.A. Bakka, M.B. Strøm, J.H. Andersen, O.R. Gautun, Synthesis and antimicrobial evaluation of cationic low molecular weight amphipathic 1,2,3-triazoles, Bioorg. Med. Chem. Lett. 27 (2017) 1119–1123.
[20] M.K. Langer, A. Rahman, H. Dey, T. Anderssen, F. Zilioli, T. Haug, H.-M. Blencke, K. Stensvåg, M.B. Strøm, A. Bayer, A concise SAR-analysis of antimicrobial cationic amphipathic barbiturates for an improved activity-toxicity profile, Eur. J. Med. Chem. 241 (2022), 114632.
[21] M.H. Paulsen, E.A. Karlsen, D. Ausbacher, T. Anderssen, A. Bayer, P. Ochtrop, C. Hedberg, T. Haug, J.U. Ericson Sollid, M.B. Strøm, An amphipathic cyclic tetrapeptide scaffold containing halogenated $\beta^{2,2}$-amino acids with activity against multiresistant bacteria, J. Pept. Sci. 24 (2018) e3117.
[22] K. Kieć-Kononowicz, K. Stadnicka, A. Mitka, E. Pękala, B. Filipek, J. Sapa, M. Zygmunt, Synthesis, structure and antiarrhythmic properties evaluation of new basic derivatives of 5,5-diphenylhydantoin, Eur. J. Med. Chem. 38 (2003) 555–566.
[23] J. Handzlik, A.J. Bojarski, G. Satała, M. Kubacka, B. Sadek, A. Ashoor, A. Siwek, M. Więcek, K. Kucwaj, B. Filipek, K. Kieć-Kononowicz, SAR-studies on the importance of aromatic ring topologies in search for selective 5-HT7 receptor ligands among phenylpiperazine hydantoin derivatives, Eur. J. Med. Chem. 78 (2014) 324–339.
[24] T.R. Rodgers, M.P. LaMontagne, A. Markovac, A.B. Ash, Hydantoins as antitumor agents, J. Med. Chem. 20 (1977) 591–594.
[25] A.A. El-Barbary, A.I. Khodair, E.B. Pedersen, C. Nielsen, S-Glucosylated hydantoins as new antiviral agents, J. Med. Chem. 37 (1994) 73–77.
[26] S. Cortes, Z.-K. Liao, D. Watson, H. Kohn, Effect of structural modification of the hydantoin ring on anticonvulsant activity, J. Med. Chem. 28 (1985) 601–606.
[27] R. Sarges, R.C. Schnur, J.L. Belletire, M.J. Peterson, Spiro hydantoin aldose reductase inhibitors, J. Med. Chem. 31 (1988) 230–243.
[28] E. Szymańska, K. Kieć-Kononowicz, Antimycobacterial activity of 5-arylidene aromatic derivatives of hydantoin, Il Farmaco 57 (2002) 355–362.
[29] E. Szymańska, K. Kieć-Kononowicz, A. Białecka, A. Kasprowicz, Antimicrobial activity of 5-arylidene aromatic derivatives of hydantoin. Part 2, Il Farmaco 57 (2002) 39–44.
[30] J. Handzlik, E. Szymańska, J. Chevalier, E. Otrębska, K. Kieć-Kononowicz, J.-M. Pagès, S. Alibert, Amine–alkyl derivatives of hydantoin: new tool to combat resistant bacteria, Eur. J. Med. Chem. 46 (2011) 5807–5816.
[31] C.J. White, A.K. Yudin, Contemporary strategies for peptide macrocyclization, Nat. Chem. 3 (2011) 509–524.
[32] X. Chen, E.G. Mietlicki-Baase, T.M. Barrett, L.E. McGrath, K. Koch-Laskowski, J. J. Ferrie, M.R. Hayes, E.J. Petersson, Thioamide substitution selectively modulates proteolysis and receptor activity of therapeutic peptide hormones, J. Am. Chem. Soc. 139 (2017) 16688–16695.
[33] M. Feng, B. Tang, S.H. Liang, X. Jiang, Sulfur containing scaffolds in drugs: synthesis and application in medicinal chemistry, Curr. Top. Med. Chem. 16 (2016) 1200–1216.

[34] S. Pathania, R.K. Narang, R.K. Rawal, Role of sulphur-heterocycles in medicinal chemistry: an update, Eur. J. Med. Chem. 180 (2019) 486–508.
[35] M.C. Bagley, J.W. Dale, E.A. Merritt, X. Xiong, Thiopeptide antibiotics, Chem. Rev. 105 (2005) 685–714.
[36] X. Just-Baringo, F. Albericio, M. Álvarez, Thiopeptide antibiotics: retrospective and recent advances, Mar. Drugs 12 (2014) 317–351.
[37] H.C. Neu, β-Lactam Antibiotics: structural relationships affecting *in vitro* activity and pharmacologic properties, Rev. Infect. Dis. 8 (1986) 237–259.
[38] E. Ware, The chemistry of the hydantoins, Chem. Rev. 46 (1950) 403–470.
[39] M. Meusel, M. Gütschow, Recent developments in hydantoin chemistry, A review, Org. Prep. Proced. Int. 36 (2004) 391–443.
[40] C.A. López, G.G. Trigo, The chemistry of hydantoins, in: A.R. Katritzky (Ed.), Adv. Heterocycl. Chem., Academic Press, 1985, pp. 177–228.
[41] L. Konnert, F. Lamaty, J. Martinez, E. Colacino, Recent advances in the synthesis of hydantoins: the state of the art of a valuable scaffold, Chem. Rev. 117 (2017) 13757–13809.
[42] W.T. Read, Researches on hydantoins. Synthesis of the soporific, 4,4-phenylethyl-hydantoin (Nirvanol), J. Am. Chem. Soc. 44 (1922) 1746–1755.
[43] H.T.L. Bucherer V A, Syntheses of hydantoins. II. Formation of substituted hydantoins from aldehydes and ketones, J. Prakt. Chem. 141 (1934) 5–43.
[44] H. Biltz, Constitution of the products of the interaction of substituted carbamides on benzil and certain new methods for the preparation of 5,5-diphenylhydantoin, Ber. Dtsch. Chem. Ges. 41 (1908) 1379–1393.
[45] C. Hulme, L. Ma, J.J. Romano, G. Morton, S.-Y. Tang, M.-P. Cherrier, S. Choi, J. Salvino, R. Labaudiniere, Novel applications of carbon dioxide/MeOH for the synthesis of hydantoins and cyclic ureas via the Ugi reaction, Tetrahedron Lett. 41 (2000) 1889–1893.
[46] C. Hulme, H. Bienaymé, T. Nixey, B. Chenera, W. Jones, P. Tempest, A.L. Smith, Library generation via postcondensation modifications of isocyanide-based multicomponent reactions, in: Methods Enzymol., Academic Press, 2003, pp. 469–496.
[47] D.V. Leusen, A.M.V. Leusen, Synthetic uses of tosylmethyl isocyanide (TosMIC), in: Organic Reactions, 2004, pp. 417–666.
[48] R. Sakata, T. Soeta, Y. Ukaji, One-Carbon homologation of pyrrole carboxaldehyde via wittig reaction and mild hydrolysis of vinyl ether - toward the synthesis of a stericcaly locked phytochrome chromophore, Heterocycles 91 (2015) 593–603.
[49] Z. Kosarych, T. Cohen, Rapid, high-yield cleavage of enol and dienol methyl ethers under mild conditions using chlorotrimethylsilane/sodium iodide, Tetrahedron Lett. 21 (1980) 3959–3962.
[50] H. Stetter, R.Y. Rämsch, Über die präparative Nutzung der 1,3-thiazoliumsalzka-talysierten Acyloin- und Benzoin-Bildung; IV1, Herstellung von Acyloinen mit funktionellen Gruppen, 1981, pp. 477–478. Synthesis, 1981.
[51] Y.B. Kim, C.S. Kim, C.K. Lee, Condensation reactions of aryl acyloins with ureas in ethylene glycol, J. Heterocycl. Chem. 31 (1994) 1653–1656.
[52] H.C. Carrington, Thiohydantoins. Part I. Preparation of 5 : 5-disubstituted 2 : 4-dithiohydantoins from the corresponding ketones, J. Chem. Soc. (1947) 681–683, 131.
[53] M. Marinov, S. Minchev, N. Stoyanov, G. Ivanova, M. Spassova, V. Enchev, Synthesis, spectroscopic characterization and *ab initio* investigation of thioanalogues of spirohydantoins, Croat. Chem. Acta 78 (2005) 9–16.
[54] G. Wenska, S. Paszyc, Photolysis of thiopurines in the presence of oxygen, Z. Naturforsch. B Chem. Sci. 36 (1981) 1628–1631.
[55] M. Terada, R. Watanabe, II.3.6 barbiturates, in: Drugs and Poisons in Humans, Springer Berlin, Heidelberg, 2005, pp. 301–313.
[56] M. Virta, K.E.O. Åkerman, P. Saviranta, C. Oker-Blom, M.T. Karp, Real-time measurement of cell permeabilization with low-molecular-weight membranolytic agents, J. Antimicrob. Chemother. 36 (1995) 303–315.
[57] J. Chatterjee, E.A. Meighen, Biotechnological applications of bacterial bioluminescence (lux) genes, Photochem. Photobiol. 62 (1995) 641–650.
[58] J. Lehtinen, M. Virta, E.-M. Lilius, Fluoro-luminometric real-time measurement of bacterial viability and killing, J. Microbiol. Methods 55 (2003) 173–186.
[59] M. Virta, K.E. Akerman, P. Saviranta, C. Oker-Blom, M.T. Karp, Real-time measurement of cell permeabilization with low-molecular-weight membranolytic agents, J. Antimicrob. Chemother. 36 (1995) 303–315.
[60] E. Juskewitz, E. Mishchenko, V.K. Dubey, M. Jenssen, M. Jakubec, P. Rainsford, J. Isaksson, J.H. Andersen, J.U. Ericson, Lulworthinone: *In vitro* mode of action investigation of an antibacterial dimeric naphthopyrone isolated from a marine fungus, Mar. Drugs 20 (2022) 277.
[61] T. Kuyyakanond, L.B. Quesnel, The mechanism of action of chlorhexidine, FEMS Microbiol. Lett. 100 (1992) 211–215.
[62] B. Loh, C. Grant, R.E. Hancock, Use of the fluorescent probe 1-*N*-phenylnaphthylamine to study the interactions of aminoglycoside antibiotics with the outer membrane of *Pseudomonas aeruginosa*, Antimicrob. Agents Chemother. 26 (1984) 546–551.
[63] M. Graf, M. Mardirossian, F. Nguyen, A.C. Seefeldt, G. Guichard, M. Scocchi, C. A. Innis, D.N. Wilson, Proline-rich antimicrobial peptides targeting protein synthesis, Nat. Prod. Rep. 34 (2017) 702–711.
[64] E. Podda, M. Benincasa, S. Pacor, F. Micali, M. Mattiuzzo, R. Gennaro, M. Scocchi, Dual mode of action of Bac7, a proline-rich antibacterial peptide, Biochim. Biophys. Acta 1760 (2006) 1732–1740.
[65] M.L. Scocchi C, P. Decarli, G. Mignogna, P. Christen, R. Gennaro, The proline-rich antibacterial peptide Bac7 binds to and inhibits *in vitro* the molecular chaperone DnaK, Int. J. Pept. Res. Therapeut. 15 (2009) 147–155.
[66] M. Mardirossian, R. Grzela, C. Giglione, T. Meinnel, R. Gennaro, P. Mergaert, M. Scocchi, The host antimicrobial peptide Bac71-35 binds to bacterial ribosomal proteins and inhibits protein synthesis, Chem. Biol. 21 (2014) 1639–1647.